# Measurement and Verification of the Voltage Distribution on High Voltage Insulators

Vassiliki T. Kontargyri, Ioannis F. Gonos, *Member, IEEE*, Ioannis A. Stathopulos, and Alex M. Michaelides

***Abstract*—The paper presents a study into the potential and electric field distribution along an insulator string, which is used for the suspension of 150 kV overhead transmission lines. In order to calculate the voltage distribution, a model of the insulator string was set up using OPERA, an electromagnetic analysis program based on the Finite Elements method. Simulation results have been compared with experiments which were successfully conducted in the High Voltage Laboratory of the National Technical University of Athens. The experimental procedure is also presented in the paper and discrepancies between simulated results and experiment and discussed.**

***Index Terms*—Insulators, electric fields, simulation software, finite element methods.**

## I. Introduction

Insulator strings are used for the suspension of overhead transmission lines. Capacitances are developed between each insulator in the insulator string with respect to the high voltage conductor as well as to earth. In addition, stray capacitances between insulators are developed. These capacitances have different values for different positions of the insulators in the string. As a result, the voltage distribution along the insulators is not uniform, with the insulators nearer the conductor are more highly stressed.

Several numerical computation methods have been developed for computing electric fields and potential in studying the behaviour of insulators [1-6]. These methods give the possibility to examine the behaviour of models with very complex geometry without using analytical methods or experiments.

In this paper, the field and potential variation in a porcelain insulator string is thoroughly investigated using modeling tools and experiment. Modelling results obtained using OPERA-2d and OPERA-3d, a software suite that uses the finite element method to solve the partia1 differential equations that describe the behaviour of electromagnetic fields, are compared with experimental results.

Manuscript received April 19, 2006. This work is co - funded by the European Social Fund (75%) and National Resources (25%) - Operational Program for Educational and Vocational Training II (EPEAEK II) and particularly by the Program HERAKLEITOS.

V. T. Kontargyri, I. F. Gonos, I. A. Stathopulos are with the School of Electrical and Computer Engineering, National Technical University of Athens, 157 80 GREECE (phone: +30-210-7722226, +30-210-7723582; fax: +30-210-7723504; e-mails: vkont@central.ntua.gr, igonos@ieee.org, stathop@ power.ece.ntua.gr).

A. M. Michaelides is with the Vector Fields, U.K., 24 Bankside, Kidlington, Oxford OX5 1JE, U.K. (e-mail: Alex.Michaelides@vectorfields.co.uk).

## II. Experimental Apparatus

The aim of the experiments was the study of the voltage distribution along an insulator string. The investigated insulator string that consists of ten porcelain insulators of the cap-and-pin type is used for the suspension of 150kV overhead transmission lines. The test arrangement is shown in Fig. 1.

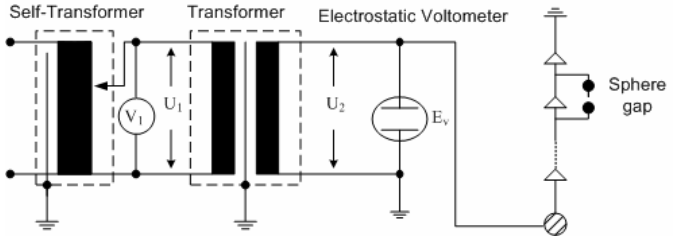


Fig. 1. Experimental set-up.

A 110V/55kV transformer is fed through a 230V self-transformer. At one edge of the insulator string (10th insulator) is connected a transmission line and the other edge (1st insulator) is grounded. The geometrical characteristics of the investigated insulator are the diameter, which is 254 mm, the height, which is 146 mm, and the creepage distance, which is 305 mm. In parallel with the i-insulator is connected a sphere gap. The high voltage is measured by two methods. The first method uses the voltmeter $V_1$ in the primary part of the transformer and then transforms the low voltage $U_1$ to a high voltage using the voltage transformer ratio (a) multiplier. The second method uses an electrostatic voltmeter $E_v$ and measures the high voltage $U_2$ in the secondary of the transformer [7, 8]. The average $U_t$ of the two values is the voltage applied across the ten insulator strings:

$$U_{ti} = \frac{U_{1i} \cdot a + U_{2i}}{2} \tag{1}$$

By increasing the voltage $U_2$, the sphere gap critical voltage $U_d$ is being reached. The percentage of the voltage $P_i$, which is applied in the *i*-insulator, is given by

$$P_i = \frac{U_d}{U_{ti}} \cdot 100\% \tag{2}$$

Moving the sphere gap in each of the ten insulators and calculating the rates $P_i$ for each insulator, the critical voltage of the sphere gap is calculated by the equation

$$\sum_{i=1}^{10} P_i = U_d \cdot \sum_{i=1}^{10} \frac{1}{U_{ti}} = 1 \qquad (3)$$

In Fig. 2 a series of experimental results is presented. The voltage distribution across the insulators is not uniform, owing to the presence of stray capacitances. It is noted that the precision of the measurements is proven from the repeatability and reproducibility of the measurement results.

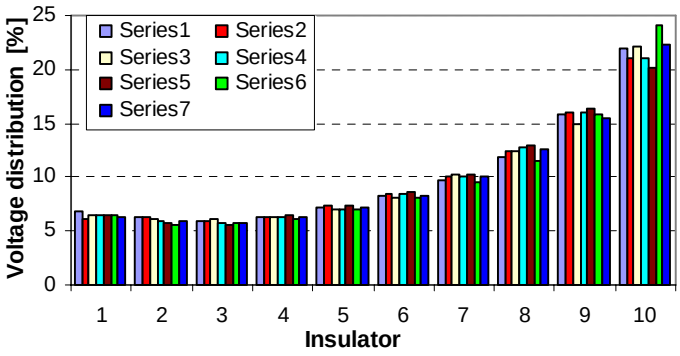


Fig. 2. Series of experimental results: Insulator Rates.

## III. Simulation

OPERA, a Finite Element Analysis program for two and three dimensional electromagnetic design [9, 10], was used to analyse fields and potentials along the insulator string. The insulator string was first modeled using OPERA-2d. The model assumes that the complete geometry is axi-symmetric. Although the assumption is true for the insulator string components, it does not provide a true representation of the excited and earth conductors. In order to increase the accuracy of the results, the density of the finite element mesh was increased in the critical regions of the insulator where the dielectric properties of the materials are such that the electric field intensity changes rapidly in space. Fig. 3 presents the potential distribution as computed in the two- dimensional model of the set-up. Fig. 4 illustrates the potential distribution along a set of lines running parallel to (and at different distances from) the axis of the insulators. Fig. 5 shows the electric field distribution along the same lines.

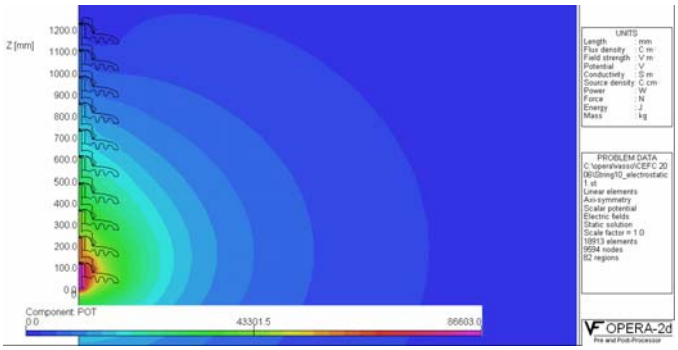


Fig. 3. Equipotential contours in and around the insulator.

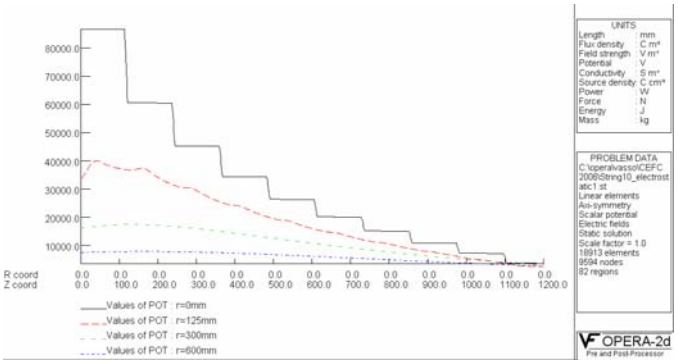


Fig. 4. Potential along the insulator.

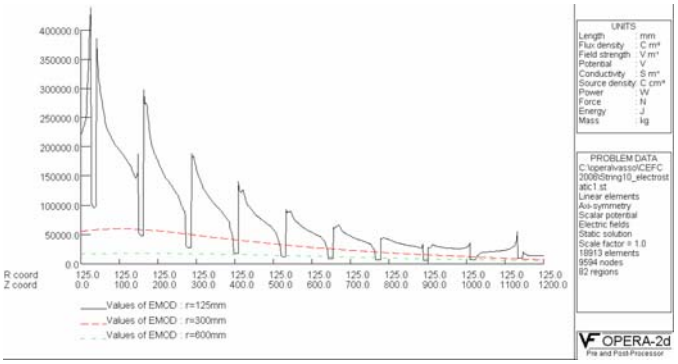


Fig. 5. Electric Field along the insulator.

The main compromise in creating a two-dimensional model of the insulator string setup related to the fact that although the main insulator geometry was axi-symmetric, the complete structure was in essence three-dimensional, owing to the presence of the excited and earth conductors [11]. In order to alleviate this, the insulator string was subsequently simulated using the three-dimensional program OPERA-3d.

Fig. 6 shows the complete three-dimensional model of the cap-and-pin insulator string structure, which is used for the suspension of 150kV overhead transmission lines.

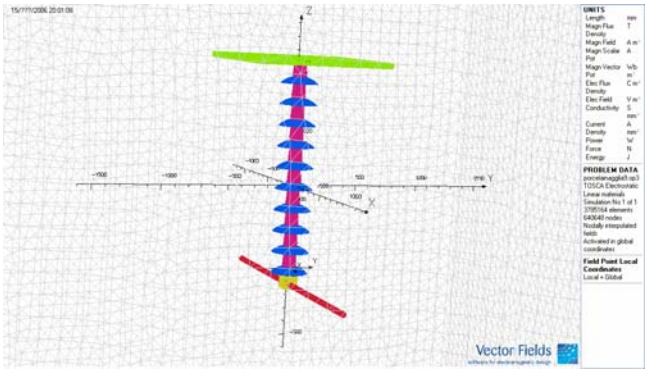


Fig. 6. The three-dimensional model of the insulator.

Figs. 7 and 8 depict the potential and electric field distribution on a cartesian patch on a YZ plane for the cap-and-pin insulator string structure (note that the insulator axis in the OPERA-3d model was maintained to be the Z-axis, with the excited conductor running along the X axis). The section

of the insulator nearer the conductor is shown to be more highly stressed.

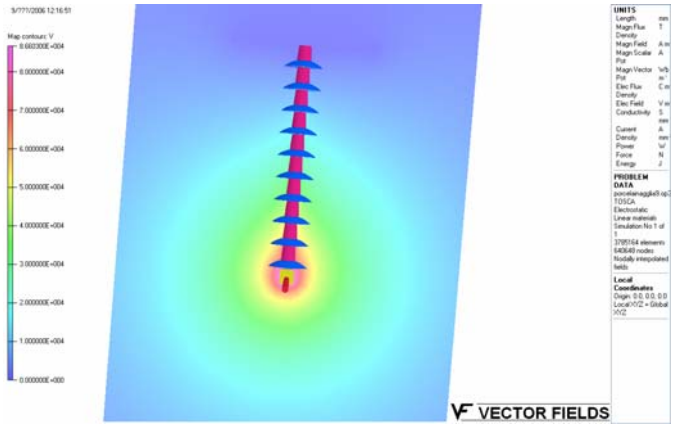


Fig. 7. Potential distribution in the porcelain insulator.

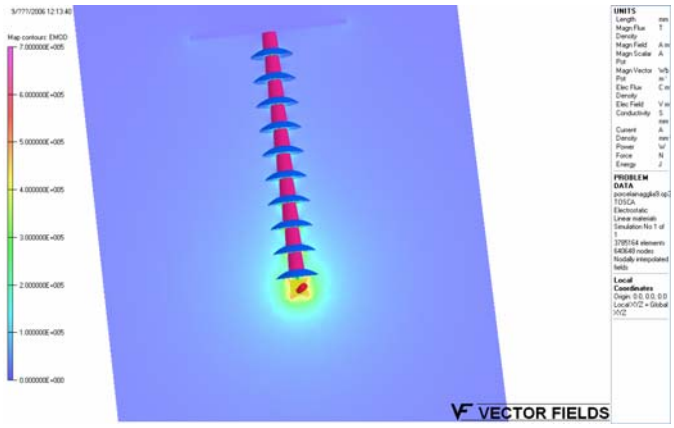


Fig. 8. Electric field distribution in the porcelain insulator.

Figs. 9 and 10 illustrate the potential and the electric field distribution, respectively, along a set of lines running parallel to the axis of the insulators (Z-axis) and at different distances from this along the Y-axis (the above lines are vertical wrt the X-axis).

Figs. 11 and 12 present the potential and the electric field distribution, respectively, along a set of lines running parallel to the Z-axis and at different distances along the X-axis.

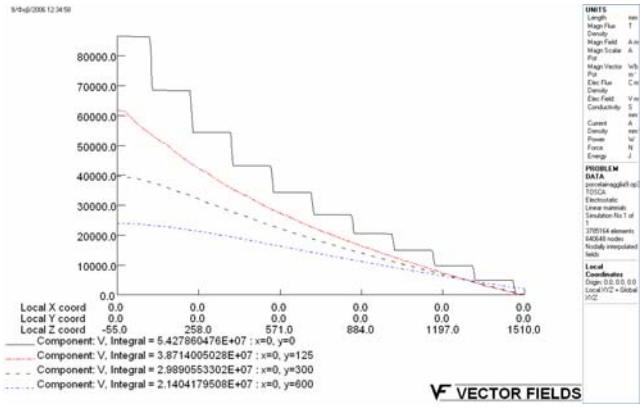


Fig. 9. Potential along lines parallel to the insulator axis and at different distances from this along the Y-axis

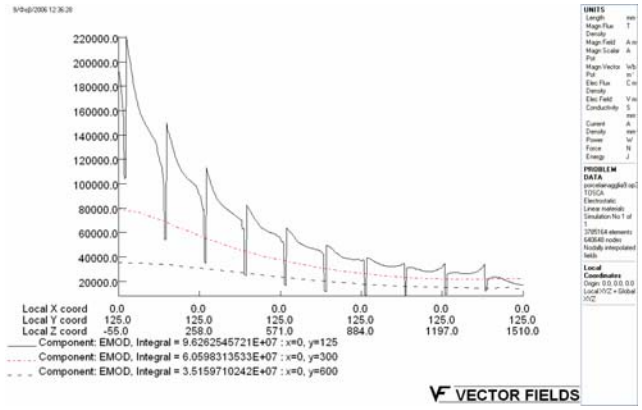


Fig. 10. Electric field along lines parallel to the insulator axis and at different distances from this along the Y-axis.

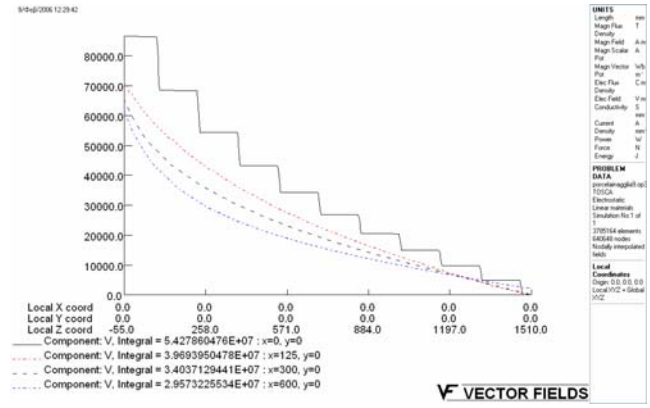


Fig. 11. Potential along lines parallel to the insulator axis and at different distances from this along the X-axis.

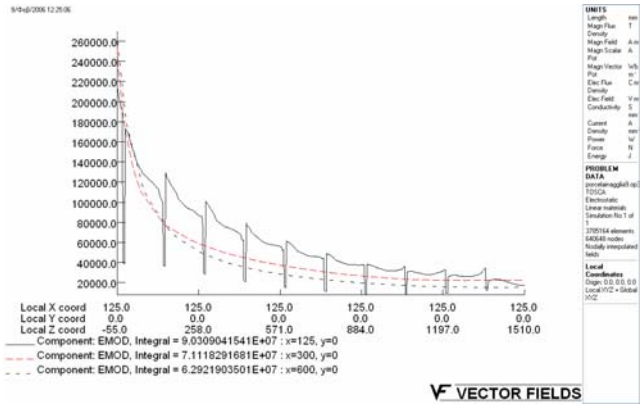


Fig. 12. Electric Field along lines parallel to the insulator axis and at different distances from this along the X-axis.

The values of the potential and the electric field in Figs. 9 and 10 are shown to be lower that those of Figs. 11 and 12, owing to the position of the excited conductor. This variation in the field around the azimuth of the insulator strings cannot be calculated using the two-dimensional model. It is hence shown that a significant error is inherent in the two dimensional model, and successfully quantified using the three-dimensional software.

Fig. 13 presents the electric field as a histogram on a cartesian patch on the YZ plane which passes through the center of the model at X=0. The insulator near the excited

conductor is more highly stressed, although the value of the electric field is still at a level lower than the dielectric stress of the porcelain.

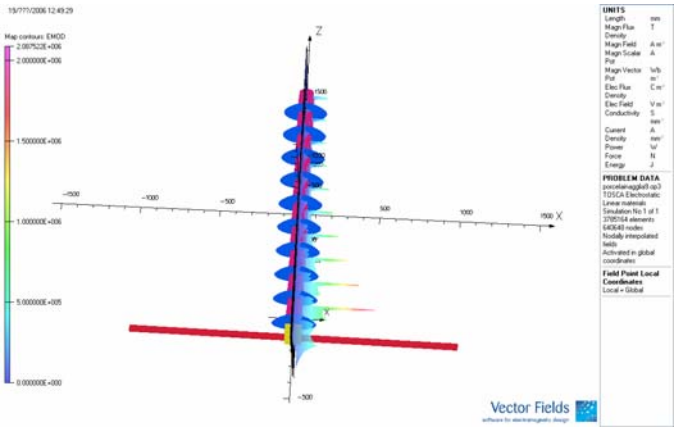


Fig. 13. Histogram of the electric field in a cartesian patch on a YZ plane at X=0.

## IV. Comparison of The Results

Fig. 14 presents a comparison of two and three-dimensional simulated results of the insulator string voltage distribution with experiment. Fifteen series of experiments have been carried out and the average value and the standard deviation have been calculated. A very good agreement has been ascertained, when comparing the experimental results with simulated OPERA-3d results. On the contrary, OPERA-2d simulation results show a significant deviation from experiment. The reason of this disagreement is attributed to the fact that the two-dimensional model cannot correctly represent how the geometry of the excited and earth conductors significantly alter the axi-symmetry of the problem.

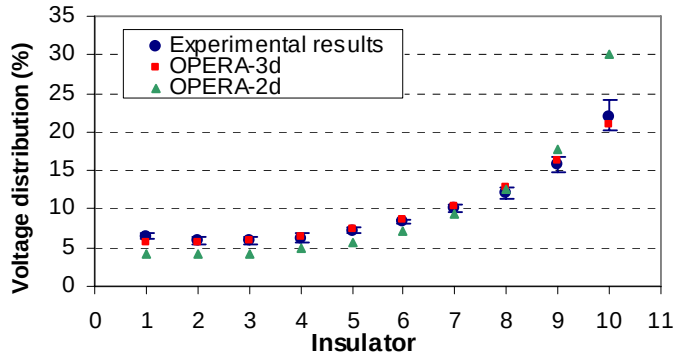


Fig. 14. Comparison between experimental and simulation results.

## V. Conclusions and Future Work

The studied approach is applicable to any insulator type, leading to reliable results in a very fast and economic way, helping the HV overhead line planners to the selection of the right insulator type. A very good agreement has been ascertained, when comparing experimental results with results from simulations using OPERA-3d. Two-dimensional model results deviate from experiment, due to the presence (and significance) of the non-symmetric parts of the model (i.e. the transmission line and ground). Although good agreement was obtained between experimental results and 3d-FEA prediction, more work is needed to achieve better, consistent agreement and account for pollution effects. The work needs to focus on obtaining accurate material data (permittivity and conductivity values) for the materials constituting the insulator (porcelain, cement and iron) as well as the pollution. It is intended to depart from conventional methods for the modeling of the insulator strings using an Electrostatics solver. The model needs to account for the conductivity of the insulator components. Having optimized the setup and the mesh of the true three-dimensional geometry, it is now intended to exploit new lossy-dielectric solvers in OPERA-3d to account for the conducting as well as the dielectric properties of the materials. Such studies are currently undertaken in two dimensions using OPERAQ-2d/LD. The present work has proved that this needs to now be extended to three dimensions.

## References

[1] J.L. Rasolonjanahary, L. Krähenbühl, and A. Nicolas, "Computation of electric fields and potential on polluted insulators using a boundary element method", *IEEE Transactions on Magnetics*, Vol. 38, No. 2, pp. 1473-1476, March 1992.

[2] E. Asenjo, N. Morales, and A. Valdenegro, "Solution of low frequency complex fields in polluted insulators by means of the finite element method", *IEEE Transactions on Dielectics and Electrical Insulation*, Vol. 4, No. 1, pp. 10-16, February 1997.

[3] N. Morales, E. Asenjo, A. Valdenegro, "Field solution in polluted insulators with non-symetric boundary conditions", *IEEE Transactions on Dielectics and Electrical Insulation*, Vol. 8, No. 2, pp. , April 2001.

[4] I. Sebestyén, "Electric-field calculation for HV insulators using domain-decomposition method", *IEEE Transactions on Magnetics*, Vol. 38, No. 2, pp. 1213-1216, March 2002.

[5] V. T. Kontargyri, I. F. Gonos, I. A. Stathopulos, A.M. Michaelidis, "Calculation of the electric field on an insulator using the Finite Elements Method", *Proceedings of the 38th International Universities Power Engineering Conference (UPEC 2003)*, Thessaloniki, Greece, September 1-3, 2003, pp. 65-68.

[6] V. T. Kontargyri, I. F. Gonos, N. C. Ilia, I. A. Stathopulos, "Electric field and voltage distribution along insulators under pollution conditions", *Proceedings of the 4th Mediterranean IEE Conference and Exhibition on Power Generation, Transmission, Distribution and Energy Conversion (Med Power 2004)*, Lemesos, Cyprus, November 15-17, 2004.

[7] IEC 60060-1, "High voltage test technique, Part 1: General Definitions and test requirements", November 1989.

[8] IEC 60060-2, "High voltage test technique, Part 1: Measuring systems", November 1994.

[9] Vector Fields, *OPERA-2d Reference Manual*, Vector Fields Limited, England, November 2004.

[10] Vector Fields, *OPERA-3d Reference Manual*, Vector Fields Limited, England, November 2004.

[11] T. Zhao, M. G. Comber, "Calculation of Electric Field and Potential Distribution Along Nonceramic Insulators Considering the Effects of Conductors and Transmission Towers", *IEEE Transactions on Power Delivery*, Vol. 15, No. 1, pp. 313-318, January 2000.